Carbohydrate Polymers 227 (2020) 115296

Contents lists available at ScienceDirect

Carbohydrate Polymers

journal homepage: www.elsevier.com/locate/carbpol

Preparation of a novel asymmetric wettable chitosan-based sponge and its role in promoting chronic wound healing

Guixue Xia[a,*], Dongqing Zhai[a], Yue Sun[a], Lin Hou[b], Xiaofan Guo[c], Lixia Wang[a], Zhijian Li[a], Feng Wang[a]

[a] College of Pharmacy, Weifang Medical University, Weifang, Shandong, 261053, PR China
[b] College of Life Science, Qilu Normal University, Jinan, Shandong, 250200, PR China
[c] College of Pharmacy, Weifang Nursing Vocational College, Weifang, Shandong, 262500, PR China

ARTICLE INFO

Keywords:
Chitosan
Asymmetric wettability
Chronic wounds
Antibacterial activity
Quaternary ammonium chitosan nanoparticles

ABSTRACT

Cutaneous chronic wounds are characterized by an impaired wound healing which may lead to infection. To surmount this problem, a novel quaternary ammonium chitosan nanoparticles (TMC NPs)/chitosan (CS)composite sponge with asymmetric wettability surfaces was successfully prepared. The optimum concentrations of TMC NPs and CS were 0.2 mg/mL and 2.0%, respectively. The incorporated TMC NPs could improve the antibacterial activity of the CS sponge. Asymmetric modification enables the CS sponge to have hydrophobic outer surface and hydrophilic inner surface. The hydrophobic surface of the sponge shows waterproof and anti-adhesion contaminant properties, whereas the hydrophilic surface preserves water-absorbing capability and efficiently inhibits the growth of bacteria. More importantly, in vivo chronic wound healing model evaluation reveals that TMC NPs/CS composite sponge promotes the wound healing and accelerates re-epithelialization and angiogenesis. And in vivo anti-infection test shows the TMC NPs/CS composite sponge could effectively prevent wound infection. These findings demonstrate that TMC NPs/CS composite sponge is a promising dressing material for chronic wounds.

1. Introduction

Skin is the largest organ of human body which acts as an anatomical barrier to protect human body from pathogens and fends, and prevent unregulated loss of body fluid. On a global scale, millions of people suffered from the loss of skin caused by excessive physical and chemical factors or diseases (Behrens, Sikorski, & Kofinas, 2014). Cutaneous wounds can be classified as chronic or acute wounds, depending on their healing tendencies. Chronic wounds are a critical healthcare issue (Mcdaniel & Browning, 2014). For instance, diabetes is one of the major risk factors for chronic wounds, for 25% diabetic patients would develop a foot ulcer (Wu, Driver, Wrobel, & Armstrong, 2007). Typically, chronic wounds are defined as those cannot achieve anatomic and functional integrity of the injured area after six weeks of standard medical treatment (Moroz & Deffune, 2013). The wounds may be exposed to infection by pathogenic bacteria during the long-term wound healing period, leading to the formation of biofilms (Sacco, Travan, Borgogna, Paoletti, & Marsich, 2015). To date, extensive research efforts have been conducted to develop wound dressing materials to hasten the healing process of chronic wounds (Ghavaminejad, Park, & Kim, 2016). Basically, a desirable wound dressing should possess gas permeability and biocompatibility. It should keep moist at the injury interface as well as act as a barrier to microorganisms (Jayakumar, Prabaharan, Sudheesh Kumar, Nair, & Tamura, 2011). Additionally, it also enlarges the body's regeneration capacity by providing support for proliferation of cells (Ong, Wu, Moochhala, Tan, & Lu, 2008).

Recently, natural polymers such as gelatin (Lee et al., 2013), collagen (Kempf, Miyamura, & Liu, 2011), silk fibroin (Schneider, Wang, Kaplan, Garlick, & Egles, 2009), cellulose (Fu, Zhang, & Yang, 2013), alginate (Murakami et al., 2010) and chitosan (Xia et al., 2016) have been employed to construct wound dressings due to their non-cytotoxicity and hydrophilicity. Synergistic compositions and novel structural design could further endow these dressings with functionality such as antimicrobial properties, growth factor or drug release abilities and biodegradable properties, thus hastening the healing process (Xia et al., 2017). Among all the materials, chitosan (CS), a polysaccharide derived from naturally abundant chitin, is currently receiving a great deal of interest for biomedical application. CS sponges have attracted significant attentions as the wound dressing due to their excellent properties, such as high porosity, high permeability, great mechanical

* Corresponding author at: College of Pharmacy, Weifang Medical University, No. 7166, Baotong West Street, Weifang, Shandong, 261053, PR China.
E-mail address: xiaguixue@hotmail.com (G. Xia).

https://doi.org/10.1016/j.carbpol.2019.115296
Received 21 April 2019; Received in revised form 20 August 2019; Accepted 5 September 2019
Available online 14 September 2019
0144-8617/

strength, large surface area and high water holding capacity (Anisha et al., 2013; Sanad & Abdel-Bar, 2017). CS has bacteriostatic properties because of the presence of amino groups. (Kong, Chen, Xing, & Park, 2010). Unfortunately, in solid state, less surface amino groups were exposed to the surface of the CS sponge, thus the bacteriostatic activity of the CS sponge was poor, which could not meet the requirements of chronic wound dressing material. CS scaffolds incorporated with nanometallic components have immense potential in the area of wound dressings due to its antimicrobial properties. Extensive studies have been done on silver (Ag) nanoparticles (Masood et al., 2019), zinc oxide (ZnO) nanoparticles (Khorasani, Joorabloo, Moghaddam, Shamsi, & MansooriMoghadam, 2018) or copper (Cu) nanoparticles (Hernandez-Rangel et al., 2019) as alternatives to antibiotics incorporated into CS scaffolds for preventing and controlling bacterial infection. However, concerns regarding the possible environmental and health impacts prevail in the use of metallic nanoparticles, which calls for a detailed evaluation of cytotoxicity. Metal-based nanoparticles (NPs) are showing certain toxicity, even if the same material is relatively inert in its bulk form (e.g., Ag, Au, and Cu). NPs also interact with proteins and enzymes within mammalian cells and they can interfere with the antioxidant defense mechanism leading to reactive oxygen species generation, the initiation of an inflammatory response and perturbation and destruction of the mitochondria causing apoptosis or necrosis (Schrand et al., 2010).

Quaternary ammonium chitosan (TMC), which is prepared by introducing a quaternary ammonium group on a dissociative hydroxyl group of CS, exhibits improved water solubility and stronger antibacterial activity relative to CS over an entire range of pH values (Tan, Ma, Lin, Liu, & Tang, 2013). TMC displays higher capability to form nanoparticles by crosslinking with negatively charged tripolyphosphate (TPP). TMC nanoparticles (TMC NPs) can not only be used as the bacteriostatic agents but also protect the incorporated active agents from premature degradation, and can provide controlled-release properties for loaded bioactive compounds (Béduneau, Saulnier, & Benoit, 2007). Hence, we decided to replace metal-based NPs with TMC NPs incorporated into CS scaffolds to enhance the bacteriostatic activity of CS.

Some studies have shown that the asymmetric super-hydrophobic/super-hydrophilic of materials is demonstrated with self-cleaning, antibacterial, self-healing and UV-blocking performance (Sasaki, Tenjimbayashi, Manabe, & Shiratori, 2016; Shen et al., 2012). The wound dressing with asymmetric surface wettability is of great interest in wound healing. The hydrophobic surface could effectively prevent external liquid including water, blood, beverages, and bacteria from contaminating the dressing. The hydrophilic surface could preserve the comfortable, moist environment to promote wound healing (Li et al., 2017; Lu et al., 2017). Recently, much attention has been paid to the coating with asymmetric properties. For examples, the reported asymmetrically wettable cotton fabrics exhibited stable ultrawater-repellent property on the one side and good water absorbing capability on the other side (Ivanova & Philipchenko, 2012; Liu, Xin, & Choi, 2012). However, their antibacterial property was not mentioned. The stearic acid modified asymmetric wettable AgNPs/chitosan exhibited the abilities of self-cleaning and antibacterial adhesion, but the use of metal-based nanoparticles is not satisfied (Liang, Lu, Yang, Gao, & Chen, 2016). Meanwhile, the effect of CS concentration on the properties of CS sponges was not mentioned. And few studies have been conducted on wound dressing materials for chronic infected wounds.

In order to obtain a satisfied wound dressing, the TMC NPs/CS composite sponge with asymmetric wettability was prepared through a simple three-step method. First, the appropriate concentration of CS sponge was screened through the physicochemical properties. Second, TMC NPs were assembled into the CS sponge which was prepared by lyophilization. And then, one side of the sponge was modified by a thin layer of stearic acid (SA). Asymmetric modification enables CS sponge to have hydrophobic outer surface and hydrophilic inner surface. The hydrophilic inner surface has the function of anti-bacterial activity and promoting wound healing. The hydrophobic outer surface has the functions of waterproofness and anti-invasion of pollutants. The TMC NPs/CS sponge is made from CS, which has the advantages of biocompatibility, non-antigenicity, non-toxicity and accessibility. On the inner surface of the composite sponge, no new compounds are introduced which can effectively reduce the penetration of harmful substances into the wounds. The incorporated TMC NPs could improve the antibacterial activity of CS sponge. TMC NPs were selected as the bacteriostatic agents for their bacteriostatic effect and biocompatibility, also they can reduced the use of antibiotics which could lead to bacterial resistance. At the same time, NPs can act as the potential drug delivery carriers.

In this study, the TMC was synthesized, TMC NPs were formed and the particle shape, size, zeta potential and antibacterial activities of NPs were studied. The effects of concentrations on the physicochemical properties (water vapor transmission rate, degradation, mechanical properties, porosity and water absorption and retention ability) of CS sponges were also studied. The waterproofing property and bacteria infiltration activity of the TMC NPs/CS composite sponge were evaluated. The TMC NPs/CS composite sponge biological properties were characterized, including cytotoxicity and antibacterial activity. A full thickness excision model of diabetic rat was used as the chronic wound model and the wound healing ability of the TMC NPs/CS composite sponge was evaluated. And the mechanisms of actions in chronic wound healing were studied. At the same time, the anti-infection ability of the TMC NPs/CS composite sponge *in vivo* was also assessed.

2. Materials and methods

2.1. Materials

Chitosan (MW: 500 kDa, DD: 90%) was purchased from Laizhou Haili Biological Product Co., Ltd (Shandong, China). Stearic acid ($CH_3(CH_2)_{16}COOH$), Methyl iodide (CH_3I), dimethyl sulfoxide (DMSO), Dulbecco's modified Eagle's medium (DMEM), thiazolyl blue tetrazolium bromide (MTT) and D'Hanks Buffer were obtained from Huasheng Biotechnology Co., Ltd. All other chemical agents were analytical grade.

2.2. Preparation and characterizations of TMC NP_S

2.2.1. Preparation of TMC NP_S

TMC was synthesized by CS with CH_3I under alkaline conditions. In detail, 1 g of CS was added to a mixture solution (20 mL of DMSO and 6 mL of 15% (w/v) NaOH solution). After 10 min, CH_3I was added and the reaction mixture was refluxed at 60 °C for 2 h. CH_3I as the reactant reacted with CS and DMSO was as the reaction solvent. The reaction of CH_3I with CS was carried out under alkaline conditions. NaOH provided an alkaline environment for the reaction. At the end of the reaction, ethyl alcohol was added to get the precipitation. The precipitation was dissolved in water and dialyzed with dialysis bag with a rejection molecular weight of 8000–14000 Da. The solution in the dialysis bag was then lyophilized to obtain TMC (Vallapa et al., 2011; Zhou et al., 2018).

The Fourier transform infrared spectroscopy (FTIR) spectra were achieved from the discs containing 2 mg of TMC samples in approximately 100 mg of potassium bromide with the frequency range from 4000 to 400 cm^{-1} at a data acquisition rate of 2 cm^{-1} per point. FTIR spectra were obtained using an infrared spectrophotometer (Nicolet 6700 FTIR Spectrometer, Thermo Fisher, USA).

^1H NMR spectrum of TMC was recorded on a 600 MHz spectrophotometer (AVANCE AV600Bruker, Germany) at room temperature and tetramethylsilane (TMS) as an internal standard. ^1H NMR sample was prepared in D_2O with concentrations of 20 mg/mL.

TMC NPs were prepared by ionic cross-linking using TPP as the cross-linker. In brief, TMC was dissolved in triple distilled water at

predetermined concentration. TMC NPs were prepared by adding TPP solution (1 mg/mL) drop wise to TMC solution (pH 7.0) under constant stirring (5000 rpm) for around 1 h resulting in the formation of turbid nano-suspension.

The particle size and zeta potential of the TMC NPs were analyzed by photon correlation spectroscopy using nano ZS90 Zeta-sizer (Malvern Instruments, UK) at a detector angle of 90°, 670 nm, and 25 °C. The samples were prepared with deionized water at appropriate concentrations. Each sample was repeatedly measured three times (Wang et al., 2016).

The morphology of the TMC NPs was observed via a transmission electron microscopy (TEM, JEM-1200EX JEOL Ltd., Japan). Briefly, a drop of sample suspension was placed onto a carbon-coated copper grid. After 2 min, the drop was taped with a filter paper to remove surface water and then air-dried before observation (Gao et al., 2016).

2.2.2. The optimization concentration of TMC NPs

The minimum inhibitory concentration (MIC) values of TMC NPs were determined against *Escherichia coli* (*E. coli*) and *Staphylococcus aureus* (*S. aureus*) using a broth dilution method. The bacterial cultures were grown overnight in liquid nutrient medium at 37 °C and diluted appropriately. The serial concentrations of TMC NPs were incubated for 24 h in a shaking incubator at 37 °C. Control group (without the addition of TMC NPs) was also conducted. These resultant suspensions (100 μL) were spotted on agar plates and incubated for 24 h. The colonies were calculated by the plate count method. The antibacterial rate was defined (Xia et al., 2017):

$$\text{The antibacterial rate (\%)} = (N_a - N_b)/N_a \times 100$$

Where N_a and N_b are the average values of colonies of the control group and the experimental groups, respectively. MIC was the one which the bactericidal rate reached more than 99.9%.

in vitro cytotoxicity of TMC NPs was investigated by the MTT assay using L929 cells. L929 cells were cultured in MEM medium supplemented with 10% fetal bovine serum at 37 °C in 5% CO_2. The cells were seeded on 96-well plates at a density of 1×10^4 cells per well and cultured for 12 h. Subsequently, the medium was replaced with different concentrations of TMC NPs. The culture medium was used as the control. The plates were incubated at 37 °C, 5% CO_2 and 95% relative humidity for 24, 48 and 72 h. At the end of the incubating, MTT (10 μL) was added and the plates were incubated for an additional 4 h. Supernatants were removed and the formazan salts were dissolved followed by addition of 150 μL DMSO on a shaking water bath at 37 °C for 10 min. The absorption values were measured at 490 nm. The relative growth rate (RGR) was expressed by the following equation (Xia et al., 2017):

$$\text{RGR (\%)} = OD_{test}/OD_{control} \times 100$$

Where OD_{test} and $OD_{control}$ are the absorption values of the test samples and the control group at 490 nm, respectively.

2.3. Preparation of CS sponges

CS was dissolved in 1% (v/v) acetic acid (Ac) solution with continuous stirring under room temperature to obtain the CS-Ac solution (0.5%, 1%, 2% and 3%, w/v), 1.5 mL solution were poured into each well of polystyrene 12-well plates (Corning, Inc.; CS016-0092; USA), frozen at −20 °C for 12 h. After that, the frozen samples were lyophilized for 24 h, then immersed in 2% NaOH (w/w) solution for 2 h. Finally, the samples were rinsed with deionized water to neutral to obtain chitosan sponge and named as CS sponge.

2.4. Preparation of asymmetrically wettable TMC NP_S/CS composite sponges

The as-prepared CS sponge was soaked into the as-prepared TMC NP_S for 24 h, frozen at −20 °C for 12 h. After that, 1 mL of stearic acid solution (20 mmol/L in alcohol) was poured uniformly onto one surface of some frozen sponges separately and kept the dressings freezing at −20 °C for 12 h. The others were untreated with stearic acid solution. After that, the frozen samples were lyophilized for 24 h to get the asymmetrically wettable TMC NP_S/CS composite sponges, which is also called modified TMC NPs/CS composite sponge (Liang et al., 2016). The sample without stearic acid treated is called TMC NP_S/CS sponge as the control.

2.5. Characterization of the sponges

2.5.1. Scanning electron microscopy (SEM)

The sponges were fixed with carbon and metalized with evaporated gold. The microstructures of the sponges were examined using a SEM (JSM-810, JEOL Ltd, Japan) as reported in a published literature (Bao et al., 2018). The acceleration voltage was set at 10.0 kV, and a magnification of 400× was used for analysis.

2.5.2. Asymmetric wettability measurement

The wettability of the CS sponge was measured via sessile drop contact angle measurements with surface tension mete (Kruss DSA100) at room temperature. At five different positions, a water droplet of 4 μL was dispensed onto the surface of sponge and the contact angle was measured.

2.5.3. Water vapor transmission rate (WVTR)

The water vapor transmission rate (WVTR) of the sponges was determined according to the American Society for Testing and Materials (ASTM International, 2016) method E96/E96M-16 (2016). The water method was employed to measure the moisture vapor transmission rate simulating the exudative wound microenvironment. Briefly, the samples were applied to seal the mouth of glass bottles containing a fixed volume of deionized water. A stagnant air gap of < 1 mm was maintained below the sample. The glass bottles were kept in hermetically closed chambers containing saturated NaCl solution to maintain a relative humidity of 75% at 37 °C. A glass bottle without any covering was used as a blank control. The systems were weighted after 24; 48 and 72 h. All experiments were performed in triplicate. The WVTR ($g/m^2/d$) was calculated according to the following equation (Lima et al., 2019):

$$\text{WVTR} = \Delta W/T/A$$

Where ΔW is the mass change in grams, T is the time during which ΔW occurred in hours and A is the permeation area of sample in m^2.

2.5.4. In vitro degradation

The degradation of sponges was examined based on the weight loss with time. In brief, the sponges were immersed into the PBS solution (pH 7.4) containing 50 mg/mL of lysozyme enzyme (15,000 U/mg) at 37 °C for 5 days. At each predetermined interval (1, 2, 3 and 5 days), the immersed sponges were taken out, washed with deionized water, and freeze-dried. The degradability of the sponges was calculated using the following equation (Anbazhagan & Thangavelu, 2018):

$$\text{Degradation (\%)} = (w_0 - w_t)/w_0 \times 100$$

Where w_0 is the initial weight of sponges, w_t is the weight of sponges after freeze-drying. The degradation percentage is expressed as the mean ± standard deviation (n = 3).

2.5.5. Mechanical test

The mechanical property of CS sponges was carried out by applying

uniaxial compression using a universal testing machine (CMT6103, MTS) at room temperature, based on adaptations of ASTM International, ASTM D882 (2012). Samples were compressed up to 80% of their original length at the displacement rate of 1 mm/min. The compressive modulus of the sponge samples was calculated from the slope of the graph obtained by stress (MPa) versus strain (%) (Hu et al., 2018).

2.5.6. Porosity measurement

The porosity of the prepared sheets was determined using the reported method (Hu et al., 2018). The sponges (the weight: m_0) were immersed in absolute ethanol until they were saturated. The weight of the dressings (m_1) was measured after the immersion. The porosity was calculated by the following equation:

$$\text{The porosity (\%)} = (m_1 - m_0)/(\rho V_1 - \rho V_0) \times 100$$

Where ρ is the density of alcohol, V_0 is the volume of alcohol before immersion, V_1 is the volume of alcohol after immersion.

2.5.7. The capacity of swelling and moisture retention

The swelling characteristic of the sponge was determined by gravimetric method. The sponge (m_0) was placed in pseudo extracellular fluid (PECF) at 37 °C for 2 h. Samples were removed from the PECF, before blotted with a piece of paper for 5 s to absorb excess PECF on the surface of the sponge and then weighted (m_w). For each specimen, at least three replicates were acquired. The swelling ratio (SR) was calculated using the following equation:

$$\text{SR (\%)} = (m_w - m_0)/m_0 \times 100$$

In order to measure the moisture retention capacity of the sponge, the wet sponge was placed in a glass dryer at 37 °C, the SR was determined at specific time intervals. The moisture retention time was recorded as the value of the SR reduced to 0%.

2.6. Antibacterial activity

2.6.1. Antibacterial activity test

The antibacterial activities of the sponges against *E. coli* (gram negative) and *S. aureus* (gram positive) were determined using transwell methods. The experiment was divided into four groups: the blank not exposed to any materials as the control group; CS sponge, TMC NPs/ CS sponge, modified TMC NPs/CS composite sponge as the experimental groups. The samples were placed under the UV light 24 h for irradiation sterilization. *S. aureus* and *E. coli* were inoculated in sterilized LB broth overnight at 37 °C in a shaking incubator, respectively. The concentration of bacteria was 10^6 colony-forming units per milliliter (CFU/mL). 0.2 mL bacterial suspension containing ~10^6 CFU/mL with 1.8 mL PBS solutions was added into 12-well plates. Experimental materials were added to the transwell mounted on 12-well plates. These 12-well plates were incubated at 37 °C in a shaking incubator operating at 130 rpm for 24 h.

After the incubation period, the quantification of viable bacteria was done by serial dilution of the bacteria culture in PBS solutions followed by plating on LB agar plate. The colonies were calculated by the plate count method. Three parallels were done in the test. (Xia et al., 2017)

2.6.2. Bacteria infiltration activity test

First, the sponges were placed under the UV light for irradiation sterilization. The sterile circular pieces of the sponges were placed on LB plates with the hydrophobic surface up. Then, 100 μL of bacterial suspension (~10^6 CFU/mL) were dropped on each surface of the sponges and incubated at 37 °C for 24 h. The sponges were removed and the growth of bacteria in the plate were observed.

2.7. In vitro cytotoxicity of the composite sponges

In vitro cytotoxicity of the composite sponges was investigated by the MTT assay using L929 cells. L929 cells were cultured in MEM medium supplemented with 10% fetal bovine serum at 37 °C in 5% CO_2. The cells were seeded in 12-well plates at a density of 2×10^5 cells per well, cultured for 12 h. Subsequently, a piece of sterile sponge was placed in a well of a 12-well plate. The culture medium without any materials was used as the blank control. The plates were incubated at 37 °C and in 5% CO_2 for 24, 48 and 72 h. At the end of the incubating, the sponges were removed, MTT (200 μL) was added to each well and then the plates were incubated for an additional 4 h. Supernatants were removed and the formazan salts were dissolved followed by addition of 2 mL DMSO on a shaking water bath at 37 °C for 10 min. The absorption values were measured at 490 nm. The relative growth rate (RGR) was expressed by the following equation:

$$\text{RGR (\%)} = OD_{test}/OD_{control} \times 100$$

Where OD_{test} and $OD_{control}$ are the absorption values of the test samples and the control group at 490 nm, respectively.

2.8. In vivo chronic wound healing

2.8.1. Preparation of streptozotocin (STZ)-induced diabetic animal model

Adult male Kunming mice (35 ± 3 g) were housed and cared in air-conditioned quarters under a photoperiod schedule of 12 h light/12 h dark cycles. The mice received standard laboratory chow and tap water available ad libitum 3 weeks prior to the experiments. Diabetes was induced by intraperitoneal injections of STZ (65 mg/kg bodyweight), in citrate buffer pH 4.5. Four days after diabetes induction, blood glucose levels were measured by a glucose meter (Life Scan Inc., Milpitas, CA, USA). The animals with blood glucose levels higher than 16.7 mmol/L were considered to be diabetic.

2.8.2. In vivo wound closure

Mice were anesthetized by intraperitoneal injection of sodium pentobarbital (65 mg/kg). The dorsal hair of diabetic mice was shaved and two 1.5 cm × 1.5 cm full-thickness wounds were created on the dorsum of each mouse. The prepared wounds were covered with the CS sponges, asymmetrically wettable TMC NP_S/CS composite sponges and the sterile cotton gauze as the control, respectively. A sterilized piece of gauze was placed over the dorsum afterwards and medical tape was used to fix gauze. After applying the dressing materials, the mice were housed individually in cages at normal room temperature.

The dressing materials were changed on days 4, 7, 10, 13 and 16 after wound creation. During the changing of materials, photographs were taken and the wound area was measured. The wound areas were expressed as a percentage of their original area immediately upon wounding at day 0, using the following formula:

$$\text{Amount of wound healing (\%)} = (A_0 - A_t)/A_0 \times 100$$

Where A_0 represents the area of the initial wound and A_t is the open area of wound at the time of biopsy on days 4, 7, 10, 13 and 16 accordingly.

On days 7, 10 and 13, three of the treated mice were killed and the tissues composed of the wound bed and surrounding healthy skin were removed for histological evaluation.

2.8.3. Histological evaluation

The skin samples were dehydrated through a graded series of ethanol, embedded in paraffin. The tissues were sectioned in 3 μm thickness slices for histopathological examination by hematoxylin/eosin (H&E). The histological slices obtained were observed by optical microscopy.

2.9. In vivo anti-infection experiment

The STZ-induced diabetic mice were prepared as described in Section 2.8.1. The infection wounds were created according to the Huang's method (Huang et al., 2017). The wounds (1 cm × 1 cm) were created as described in Section 2.8.2, 50 μL *S. aureus* suspensions (~10^6 CFU/mL) were added on each wound, after the materials covered the wounds, another 50 μL of *S. aureus* suspensions were added on the materials. Then a sterilized piece of gauze was placed over the dorsum afterwards and medical tape was used to fix gauze. The dressing materials were changed on days 4, 7, 10, 13 and 16 after wound creation. During the changing of materials, photographs were taken and the wound area was measured. Meanwhile, exudate from wounds after surgery was collected using sterile swabs and cultured in 2 mL of nutritional broth at 37 °C for 4 h. Subsequently 100 μL of the suspension was spread on nutritional agar plate followed by keeping at 37 °C overnight, then the colonies were observed (Liang et al., 2016).

2.10. Statistical analyses

Each experiment was performed independently at least in triplicate. Statistical data were analyzed using SPSS 13.0. Statistical analysis of the differences between each group was tested by one-way analysis of variance, followed by the Tukey test for between-group comparisons. Data were given as mean ± SD. $p < 0.05$ was considered statistically significant.

3. Results and discussion

3.1. Characterization of TMC NPs

The FTIR spectrum of CS and TMC are shown in Fig. S1. The broad band around 3346 cm^{-1} could be attributed to the O—H and N—H stretching vibrations. The peaks at 2934, 2884 and 1651 cm^{-1} were associated with the stretching vibrations of $-CH_2$, −CH and C═O, respectively. The peak at 1481 cm^{-1} was assigned to the C—H bending of the trimethyl ammonium group (Huang, Chen, Sun, Hu, & Gao, 2006; Li et al., 2018). These indicated introduction of quaternary ammonium groups onto chitosan chain.

^{1}H NMR spectra was analyzed to further confirm the chemical structures of TMC and the peaks attributions are labeled in Fig. S2. The signals could be identified as follows: 1.97 ppm (*N*-acetyl), 2.60 ppm (H-2), 3.67–4.00 ppm (H-3–H-6), 4.35 ppm (H-b), 4.73 ppm (D_2O and H-1) and 3.27 ppm (H-a) (Chen et al., 2016). These data indicated that TMC was successfully synthesized.

TMC NPs were prepared by ionic cross-linking using TPP as the cross-linker. The NPs were found to be spherical, smooth, non-aggregated (Fig. 1B). The diameters and zeta potentials of the NPs in the well swollen state in PBS (pH 7.4) solution at room temperature were about 238.73 ± 11.64 nm and + 15.23 ± 0.55 mV, respectively.

MTT assay was applied to evaluate the effects of TMC NPs on the cytotoxicity of L929 cells (Fig. S3). The cytotoxicity of TMC NPs was enhanced significantly ($p < 0.05$) with the increase of the concentration. The L929 cells viability was 94.6% at the concentration of 0.1 mg/mL and 52.0% of 0.5 mg/mL within 24 h. There was a significant ($p < 0.05$) decrease in cell viability at high concentrations of TMC NPs (> 0.25 mg/mL). The results indicated that the TMC NPs have low toxicity at low concentrations (< 0.25 mg/mL).

The minimum inhibitory concentration (MIC) values of TMC NPs were determined against *E. coli* and *S. aureus* using a broth dilution method. The MICs of TMC NPs were 0.1 mg/mL against *E. coli* and 0.1 mg/mL against *S. aureus*. The modified polysaccharide- quaternary ammonium chitosan (TMC), which introduces permanent positively charged quaternary ammonium groups and enhances water solubility, has attracted considerable attention recently as an antibacterial agent over a broad pH range. Electrostatic interaction between the polycationic structure and the predominantly anionic components of the microorganisms play a fundamental role in antibacterial activity. The number of ammonium groups linking to the CS backbone is important in electrostatic interaction for the antibacterial activity of TMC (Tan et al., 2013). TMC NPs were formed by crosslinking TMC with TPP.

According to the cytotoxicity and MIC of TMC NPs, 0.2 mg/mL TMC NPs at which they had desirable antibacterial effect and cytocompatibility were selected for the next tests.

3.2. Preparation and characterization of the composite sponges

3.2.1. Characterization of CS sponges

The internal structures of CS sponges with different concentrations studied by SEM are shown in Fig. 1A (a1: 0.5%; a2: 1.0%; a3: 2.0%). CS sponges with different concentrations exhibited homogeneous micropore network structures. With the increasing of CS concentrations, the pore size of CS sponges decreased gradually.

3.2.2. Asymmetric wettability measurement

The asymmetric wetting behavior of the CS sponge after SA modification was assessed by water contact angle measurement shown in Fig. 1C (c1 and c2). The contact angle is an important parameter to measure the wettability of the liquid on the surface of the material. If the contact angle is less than 90°, the solid surface is hydrophilic; if the contact angle is more than 90°, the solid surface is hydrophobic (Blackwell, 2006). The modified upward surface of the sponge showed hydrophobic property against water droplets. The water contact angle of the modified surface was 137° (c1), which exhibited highly hydrophobic property. However, the water contact angle of the unmodified surface was 78° (c2). The unmodified surface showed super hydrophilic behavior and absorbed the water droplet immediately. The SEM images of the surfaces of SA modified CS sponge were shown in Fig. S4. The modified surfaces had little amount of pores, which was ascribed to the presence of stearic acid layer. The unmodified surfaces of CS sponge still presented sponge-like and interconnected micro-porous structure, which also confirmed that the SA modified CS sponge had asymmetric surfaces.

3.2.3. Water vapor transmission rate (WVTR)

WVTR is used to determine the ability to control water loss during wound healing of sponges or other dressings. It is a fundamental physical characteristic of materials intended for wound dressings and it is the property which directly controls the moisture micro-environment during wound healing (Masood et al., 2019). Sponge wound dressing materials present improved permeability properties compared with other dressing materials (Jiang, Shun-Bin Wang, & Chen, 2017). The presence of pores in the structure is excellent for the breathability of the lesion and allows appropriate control of the microenvironment moisture, promoting wound healing. Furthermore, the porous architecture provides high gas permeation and an effective protection of the wound against external contaminants and dehydration (Lima et al., 2019). The sponge that has a high WVTR, i.e. the ability to lose large extent of water vapors is not favorable as it prevents accumulation of exudates on wound area which can cause back pressure and pain sensations on wound site (Xu et al., 2016).

The WVTR values of different materials are shown in Fig. 2A. The gauze (2826 $g/m^2/d$) and 0.5% of CS sponge (2733 $g/m^2/d$) groups showed similar WVTR values, which were higher than that of 2% and 3% CS sponges groups (2176 $g/m^2/d$ and 2155 $g/m^2/d$, respectively) ($p < 0.05$). WVTR through sponges depends on both the diffusivity and solubility of water molecules in the sponge matrix. The WVTR value of the hydrophobically modified CS sponge (2%) was also measured. The WVTR value was 2175 $g/m^2/d$, which was similar to that of CS sponge (2%). The results indicated that hydrophobic modification has little effect on WVTR.

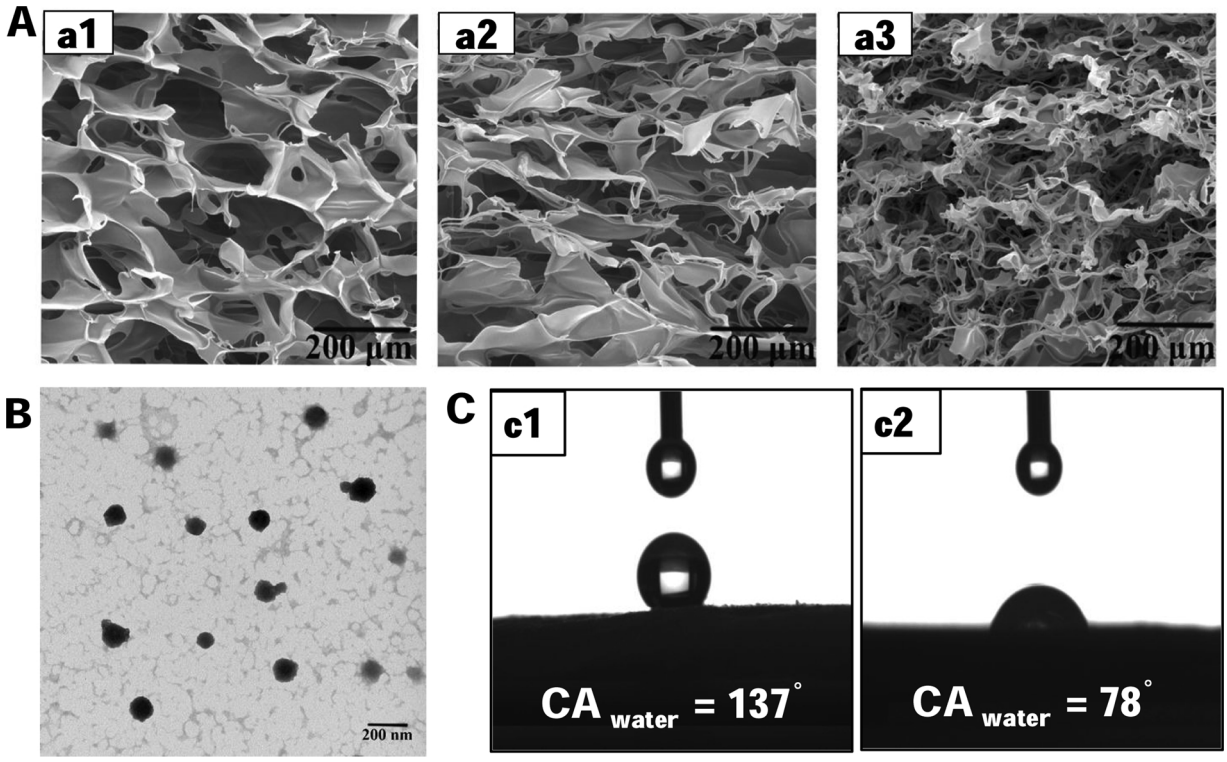

Fig. 1. A: SEM images of CS sponges (a1: 0.5%; a2: 1.0%; a3: 2.0%). B: TEM image of TMC NPs. C: Water contact angles of hydrophobic surface (c1) and hydrophilic surface (c2) of CS sponge, respectively.

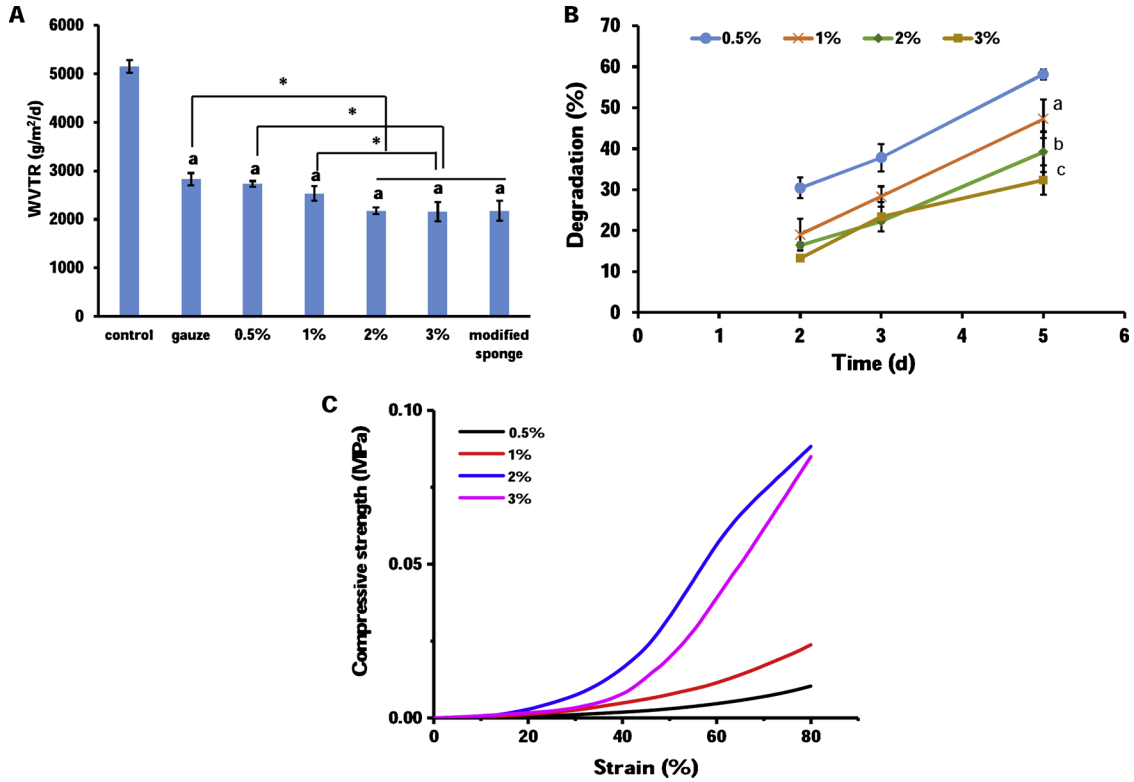

Fig. 2. A: The water vapor transmission rate (WVTR) of different materials. $^{*}p < 0.05$, $^{a}p < 0.05$ vs control group. B: *in vitro* degradation of CS sponges (0.5%, 1%, 2%, 3%). $^{a}p < 0.05$ vs 0.5% CS sponge on day 2, 3, 5. $^{b,c}p < 0.05$ vs 0.5% CS sponge on day 1, 2, 3, 5. C: Compressive strength (MPa) versus strain (%) of different concentrations of CS sponges at the displacement rate of 1 mm/min.

The dressings having a WVTR in the range of 2000–2500 g/m^2/d are ideal for maintaining optimum moisture content during wound healing. Higher WVTR would leave scars on wound surface by quick dehydration rate while low WVTR would leave the exudates on wound surface causing increase risk of bacterial growth (Queen, Gaylor, Evans, Courtney, & Reid, 1987). The CS sponges (1%, 2% and 3%) all meet the requirement of water vapor permeability, which showed that the obtained wound dressing material may provide an environment capable to improve the quality and rate of wound healing. Also, due to their WVTR values, the dressings produced could contribute in pain reduction and also in the promotion of cosmetic healing without the formation of scars.

3.2.4. In vitro degradation

The degradation profile of sponges was represented as percentage degradation as a function of time. It was reported that solvent penetrated the CS matrix, expands the lattice parameters of CS chains and causes dissociation of the hydrogen bonds between the CS chains leading to disruption of a macromolecular arrangement of CS molecules and degradation (Pawar, Bulbake, Khan, & Srivastava, 2019). The biodegradation properties of CS sponges with different concentrations were evaluated with lysozyme for 15 days. The quantification of degradation percentage is shown in Fig. 2B. The biodegradation rates of CS sponges (0.5%, 1%, 2%, 3%) were 30.4%, 19.1%, 16.5%, 13.3% (2nd day) and 58.2%, 47.3%, 39.2%, 23.8% (5th day), respectively. The results demonstrated that CS sponge (0.5%) had the highest amount of degradation ($p < 0.05$). The degradation rate increased as the concentration of CS sponges decreased. It could be attributed to the higher pore size of CS sponge (0.5%) than other higher concentrations of CS sponges, which leads to uptake of more solvent molecules. And the slower degradation rate of CS sponges (2% and 3%) may be attributed to its more compact sponge matrix. (Ordikhani, Tamjid, & Simchi, 2014; Pawar et al., 2019)

3.2.5. Mechanical properties

The mechanical properties of sponges are important requirements for the wound dressing. As a wound dressing, which requires it to be in close contact with the skin surface, and its mechanical strength needed to be tested to determine the comfort of the materials it closes to the skin surface (Fan, Yang, Yang, Peng, & Hu, 2016). When stretching out, it should not be easy to be torn. Therefore, the compressive strength of sponges were tested by compressive testing. The compressive strength of different concentrations of CS sponges is given in Fig. 2C. The compressive strengths of the 0.5%, 1%, 2% and 3% CS sponges were 0.01, 0.02, 0.09 and 0.08 MPa, respectively. The results showed that with the increase of the concentration of CS sponges (0.5%–2%), the compressive strength increased with the increase of CS sponge concentration. While the compressive strength of 3% CS sponge reduced compared with 2% CS sponge. The reason for this phenomenon can be explained as follows: with an increasing concentration of CS sponge within limits, the crosslink density of the polymer molecules increases, which effectively improves the mechanical properties of the sponge, so the compressive strength improved to a certain degree. However, the high concentration of CS increases the hardness of sponge and the sponge becomes brittle that lead to the decrease of compressive strength (Fan et al., 2016).

According to previous work, the CS sponge presents compressive strength of approximately 0.2 - 0.3 MPa (Hu et al., 2018). The compressive strength of 2% CS sponge we prepared is higher than that of the reported CS dressing, which is more sufficient for wound care application.

3.2.6. Porosity measurement

Porosity of samples was evaluated using an alcohol displacement method. It was found that the porosity of the 3% CS was the minimal (65%), the 0.5% CS showed the highest porosity (86%). As shown in Fig. 3A, with the concentration of CS increased, the porosity of sponges did not decrease significantly, but the porosity of CS sponges tended to decrease with the increase of concentration, which was consistent with SEM of CS. The high porosity of the dressing materials could benefit to absorb exudate from the wound surface, and prevent the wound infection. Furthermore, the presence of large volume of porosity is also beneficial for the transfer of nutrients and oxygen to the cells attached on the dressing materials (Li et al., 2017).

3.2.7. Swelling and moisture retention of the CS sponges

Swelling and moisture retention capability of wound dressing materials is an important property to evaluate the efficacy of clearing the wound exudate and keeping moist. The excellent swelling properties of the sponges are conduce to stop bleeding, and a moist environment can promote the healing of the wounds. The maintenance of a moist wound bed has been widely accepted as the most ideal environment for effective wound healing (Fan et al., 2016). The CS sponges absorbed large amounts of PECF, and the order of the swelling ratios for samples (2% CS sponge > 3% CS sponge > 1% CS sponge > 0.5% CS sponge) is shown in Fig. 3B. It is maybe because 3% CS sponge was too dense to reach the swelling equilibrium. And the 3% CS-Ac solution was viscous when prepared, so in the next experiment, 3% CS sponge was excluded. Compared with other composite materials previously reported in the literature (Feng et al., 2019; Kumar et al., 2010; Ma et al., 2019), the 2% CS sponge in this study showed enhanced swelling property.

The moisture retention capacity of the 2% CS sponge (longer than 12 h) is obviously longer than that of 1% CS sponge (about 7 h) and 0.5% CS sponge (about 5 h) (Fig. 3C). The moisture retention of sponge is related to its pore size. The lower porosity of sponge, the better the moisture retention capacity. The 2% CS sponge showed longer moisture retention time than other composite materials previously reported in the literature (Feng et al., 2019; Li et al., 2017). The porous surface, high and continuous liquid absorption capacity and good liquid holding ability would contributed to the high exudate absorption of the composite sponges, making them potential candidates used for wound dressing (Wang et al., 2019). In conclusion, according to the swelling and moisture retention capacities, 2% CS sponge was chosen for the next experiments.

The moisture retention capacities of asymmetrically wettable CS sponge and the unmodified CS sponge were compared. The moisture retention capacity of the asymmetrically wettable sponge is obviously longer than that of unmodified sponge. The moisture retention time of the 2% CS sponge is a little more than 12 h, whereas it is more than 24 h for the modified CS sponge (Fig. 3D). The longer moisture retention time of asymmetrically wettable CS sponge is attributed to its highly hydrophobic surface, which could effectively retard the evaporation of liquid from the inner of the sponge. According to the moist wound healing theory, moist wound treatment could promote wound healing, remove the dressing painlessly without destroying fresh formed tissue and reduce scar formation (Hinman & Maibach, 1963).

3.3. Antibacterial activity

3.3.1. Antibacterial activity test

Escherichia coli (*E. coli*) and *Staphylococcus aureus* (*S. aureus*) were used to study the antibacterial activities of CS sponge, TMC/CS sponge and hydrophobically modified TMC NPs/CS composite sponge. The survival population of *E. coli* was about 10^5 CFU/mL in TMC NPs/CS sponge and hydrophobically modified TMC NPs/CS composite sponge groups, whereas approximately 10^7 CFU/mL in CS sponge group and 3×10^7 CFU/mL in the control group (Fig. 4). The survival population of *S. aureus* was about 10^8, 4×10^7, 1.5×10^6, 10^6 CFU/mL after treated with PBS, CS sponge, TMC NPs/CS sponge and hydrophobically modified TMC NPs/CS sponge, respectively (Fig. 4). The TMC NPs/CS sponge had significant antibacterial activity (> 99.9% reduction), compared with the CS group and the control group. Hydrophobic

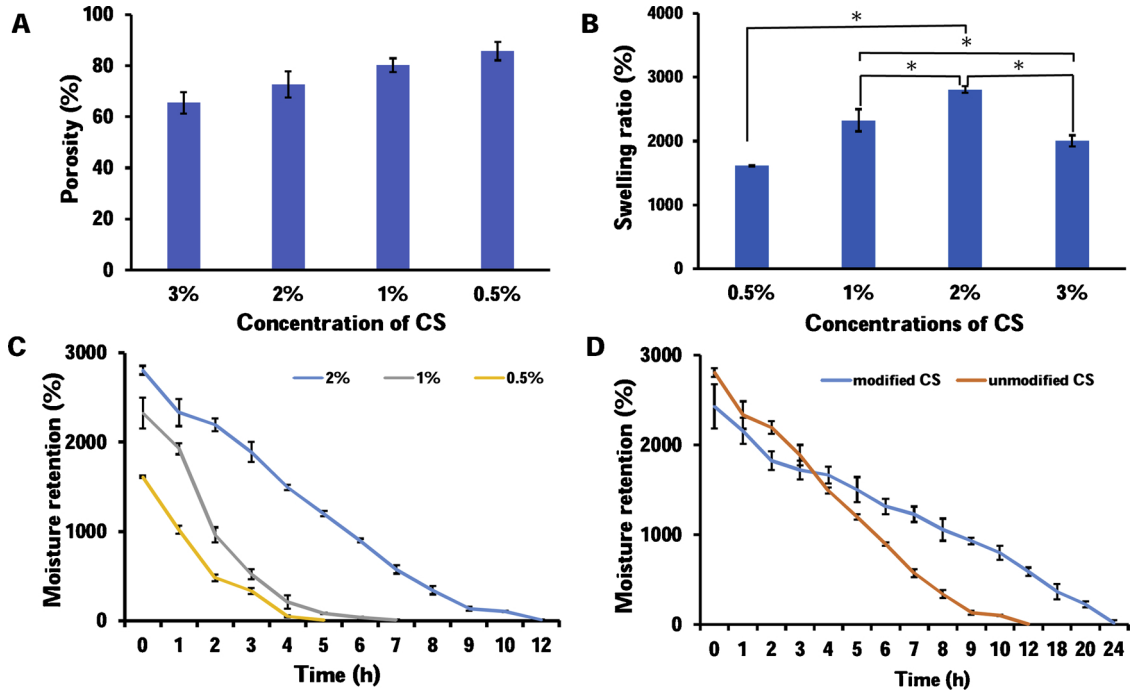

Fig. 3. A: Porosity of CS sponges; B: Swelling ratio of CS sponges; C: Moisture retention capacity of CS sponges; D: Moisture retention capacity of modified CS sponge. The results were expressed as mean ± SD (n = 3, $*p < 0.05$).

modification has little effect on the bacteriostatic activity of the TMC NPs/CS sponge.

Electrostatic interaction between the polycationic structure and the predominantly anionic components of the microorganisms plays a fundamental role in antibacterial activity (Tan et al., 2013). The amino groups of CS are the main group for the inhibition of bacterial growth (Kong et al., 2010). In solid state, less surface amino groups are exposed to the surface of the CS sponge, so the bacteriostatic activity of the CS sponge is poor. TMC is a derivative of CS by introducing ammonium groups linking to the CS, which is important in electrostatic interaction for the antibacterial activity. After quarternization, CS derivates exhibited better water solubility and stronger antibacterial activity as compared to CS (Xie, Liu, & Qiang, 2007). TMC NPs were formed by crosslinking TMC with TPP. The zeta potentials of the NPs were + 15.23 ± 0.55 mV, which indicated that a large number of amino groups were on the surface of TMC NPs, so TMC NPs still retained the bacteriostatic activity of TMC. Therefore, the addition of TMC NPs significantly enhanced the antibacterial activity of CS sponges.

3.3.2. Bacteria infiltration activity test

The result of the bacteria infiltration of the CS, SA modified CS and SA modified TMC/CS composite sponges are shown in Fig. 4B. 100 μL of bacterial suspension (*E. coli* and *S. aureus*) were dropped on each surface of the sponges. After 24 h incubation, the bacterial suspension penetrated into the CS sponge completely, while the amount of bacterial suspension penetrating into the modified CS and modified TMC/CS composite sponges is less (B1 and B3) The sponges were removed and the bacteria growth on the agar plate were observed (B2 and B4). The number of colonies growing on the agar plate was the highest in CS group, followed by modified CS group and the lowest in modified TMC/

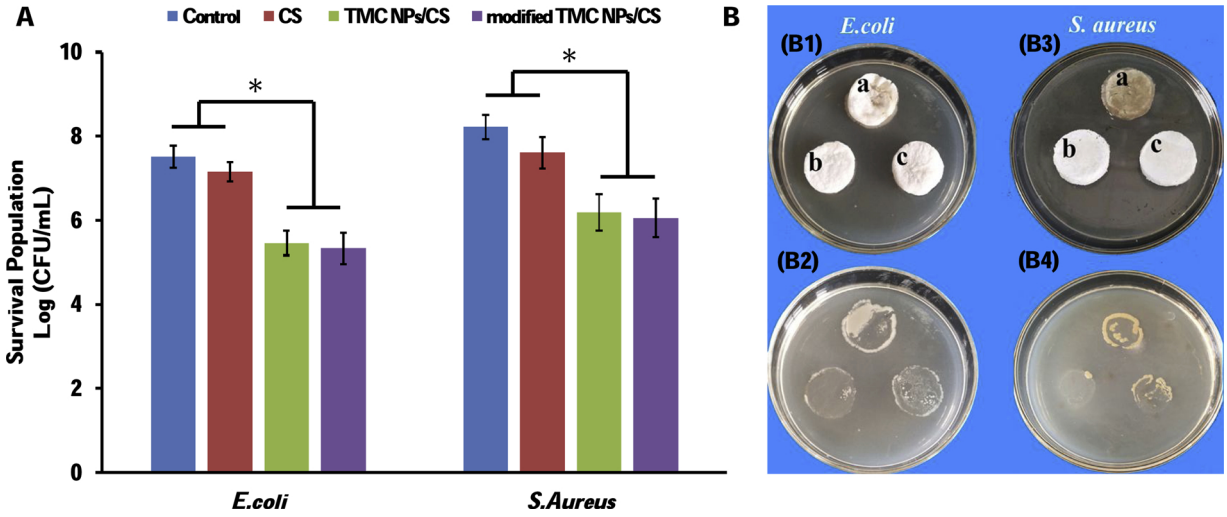

Fig. 4. A: The antibacterial activity of CS, TMC NPs/CS, modified TMC NPs/CS sponges against *E. coli* and *S. aureus*. The results were expressed as mean ± SD (n = 3, $*p < 0.05$). B: Bacteria infiltration activity of CS (a), modified TMC NPs/CS (b) and modified CS (c) sponges against *E. coli* ((B1) and (B2)) and *S. aureus* ((B3) and (B4)).

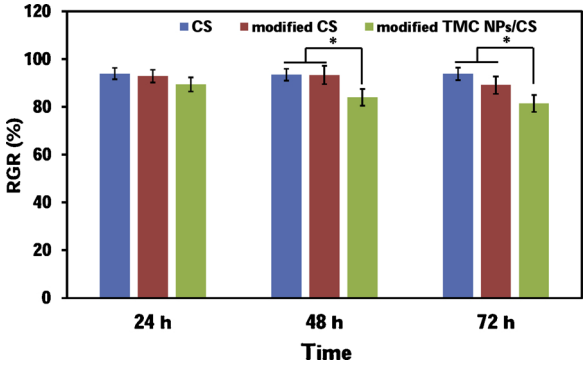

Fig. 5. Cell viability measured by MTT assay for CS, modified CS, modified TMC NPs/CS sponges after 24, 48 and 72 h of incubation. Data are presented as the mean ± SD (n = 5, *$p < 0.05$).

CS group. As can be seen from the results, a certain amount of bacterial suspension penetrated into the agar plate. Meanwhile, the addition of TMC NPs into CS sponge also effectively inhibited the proliferation of bacteria. It illustrates that the asymmetric wettability modified TMC NPs/CS composite sponge possesses both excellent infiltration resistance and antibacterial activity towards the bacteria compared with the CS and modified CS sponges.

3.4. In vitro cytotoxicity test

The cytotoxicity of composite sponges was evaluated by MTT assay using L929 cells. The relative growth rates (RGR) of L929 cells treated with CS, modified CS and modified TMC NPs/CS sponges were higher than 80% (Fig. 5). After 48 h and 72 h incubation, the relative growth rates of CS and modified CS sponge groups were higher than that of modified TMC NPs/CS group ($p < 0.05$). During the incubation, TMC NPs were released from the modified TMC NPs/CS. Due to the light cytotoxicity of TMC NPs towards L929 cells (Fig. S3), the relative growth rate of modified TMC NPs/CS group was lower that other

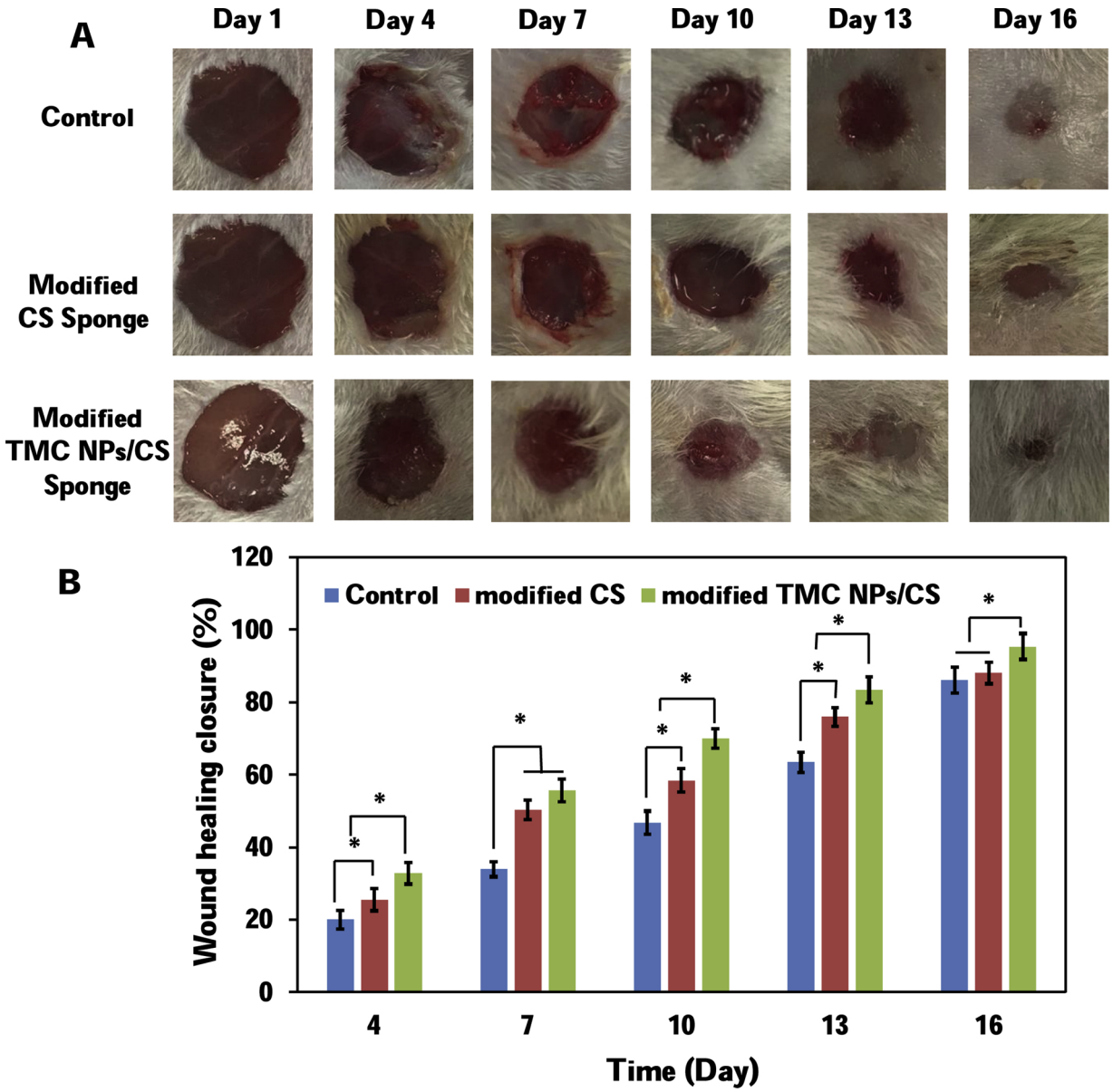

Fig. 6. *in vivo* study of healed wounds. Representative wound images of visual appearance (A) and wound area closure (%) (b) in diabetic mice on days 4, 7, 10, 13 and 16 for each treatment regimen. The results were expressed as mean ± SD (n = 3, *$p < 0.05$).

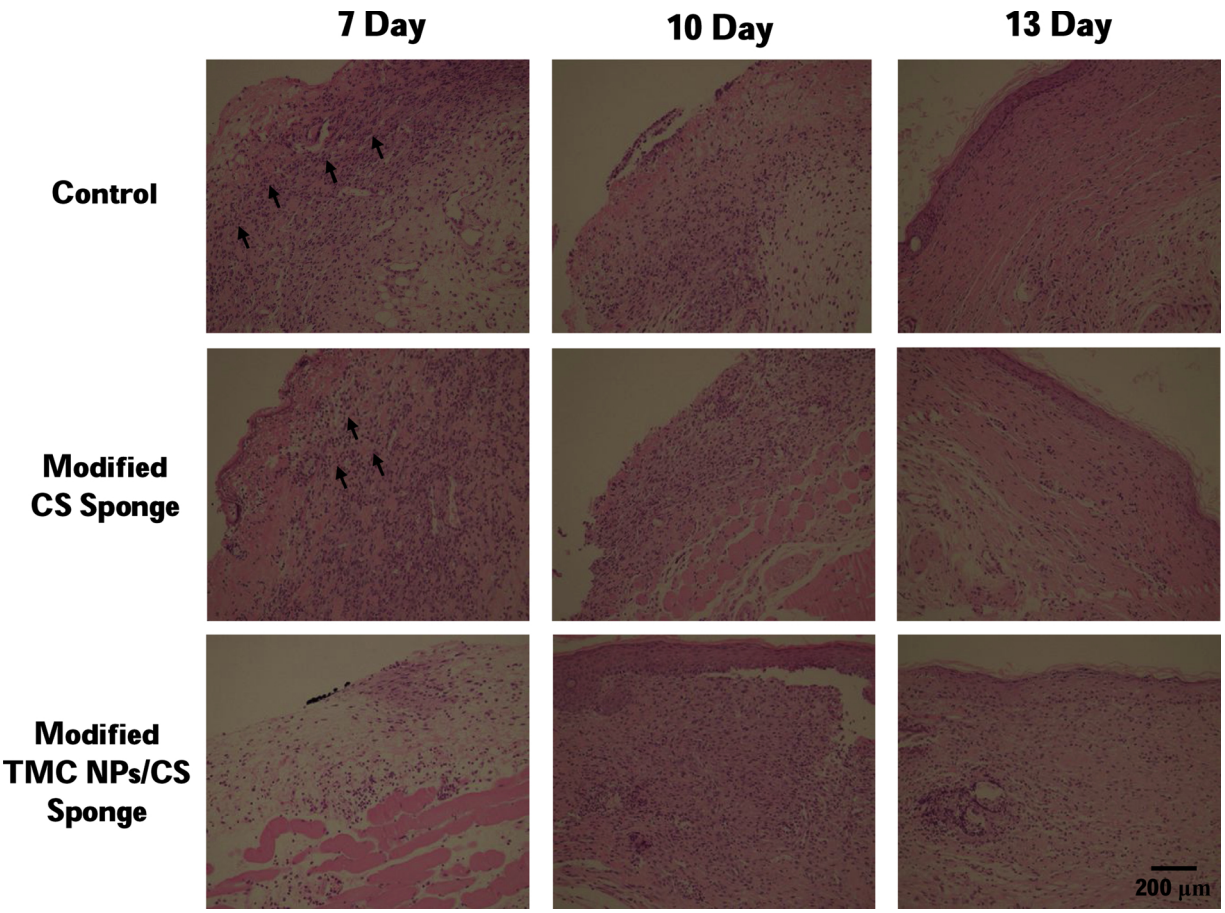

Fig. 7. Histological analysis of wounds treated with grauze, CS sponge and modified TMC NPs/CS sponge by H&E staining (magnification 200×). Black arrows indicate inflammatory cells.

groups. As reported by ISO 10993-5 (ISO, 2009), percentages of cell viability above 80% are considered as non-cytotoxic. The results indicated that the modified TMC NPs/CS sponge has no toxicity making it excellent material for wound dressing.

3.5. In vivo chronic wound healing test

3.5.1. In vivo wound closure

To determine the wound healing ability of the tested materials, macroscopic images of full thickness wounds were taken using a digital camera in diabetic mice wound models at 1, 4, 7, 10, 13 and 16 days (Fig. 6A). The percentage of the wound size remaining exposed was determined via comparing the size of the wound at each time point with the size of the wound on day 1 (Fig. 6B). CS have been reported to enhance wound healing, which can indirectly enhance cell proliferation *in vivo* (Azuma et al., 2015). Additionally, immediate migration of polymorphonuclear cells (PMN) and mononuclear cells (MN) was observed after application of CS. The PMN and MN degrade CS into its low molecular weight oligomers and monomers which exhibit strong ability for promoting cell migration (Minami, 1997). TMC showed antibacterial activity and could significantly enhanced wound re-epithelialization and contraction as the wound dressing material (Zhou et al., 2016). All the wounds treated with modified TMC NPs/CS composite sponge healed better than the CS sponge and control treatment groups. On days 4 and 7, adhesions were caused between the gauze and the wounds in the control and CS groups which resulted in wounds secondary injured during the changing dressing materials. This was due to the higher water absorption and moisture retention capacity of surface hydrophobically modified TMC NPs/CS which is conducive to preserve nutrients and keep the wound moist.

On day 5, the wounds treated with modified TMC NPs/CS sponges achieved closure to 32.8 ± 2.9% ($p < 0.05$), compared with modified CS sponge and gauze treated wound, which only showed 25.5 ± 3.1% and 20.0 ± 2.5% wound closure, respectively. A significant increase in wound area closure was evident on day 10 post-wounding with modified TMC NPs/CS sponge (70.0 ± 2.6%, $p < 0.05$) and CS sponge (58.5 ± 3.2%, $p < 0.05$), compared with control wounds (63.5 ± 3.2%). Furthermore, there was significant increase in percentage of wound area closure on day 13 in modified TMC NPs/CS (83.4 ± 3.5%) and modified CS (76.0 ± 2.6%) groups compared with the control group (63.5 ± 2.8%). On day 16, the wounds were nearly complete repaired in the experimental groups, while about 15% and 10% of the wounds were not healed in the control and modified CS group, respectively. After 13 days, hair had grown around the wound in the modified TMC NPs/CS group compared with the control group.

3.5.2. Histological evaluation of the wounds

The wound healing results were further substantiated by histological analysis of the specimens collected. Specimen sections were stained using H&E staining. Microscopic histological assessment was carried out to investigate the quality of the healing process through the quantitative investigation of several parameters such as epithelization, granulation tissue and inflammatory cells.

H&E staining of dissected tissues from each of the treated animal groups is shown in Fig. 7. At day 7 post-wounding, the inflammatory cells were less recruited to the wound site treated with modified TMC NPs/CS sponge compared with the control and CS sponge. TMC NPs had a strong bactericidal effect and the hydrophobically modified surface could prevent bacteria from reaching the wounds. As a result, less bacteria needed to be cleared in the wounds and less inflammatory

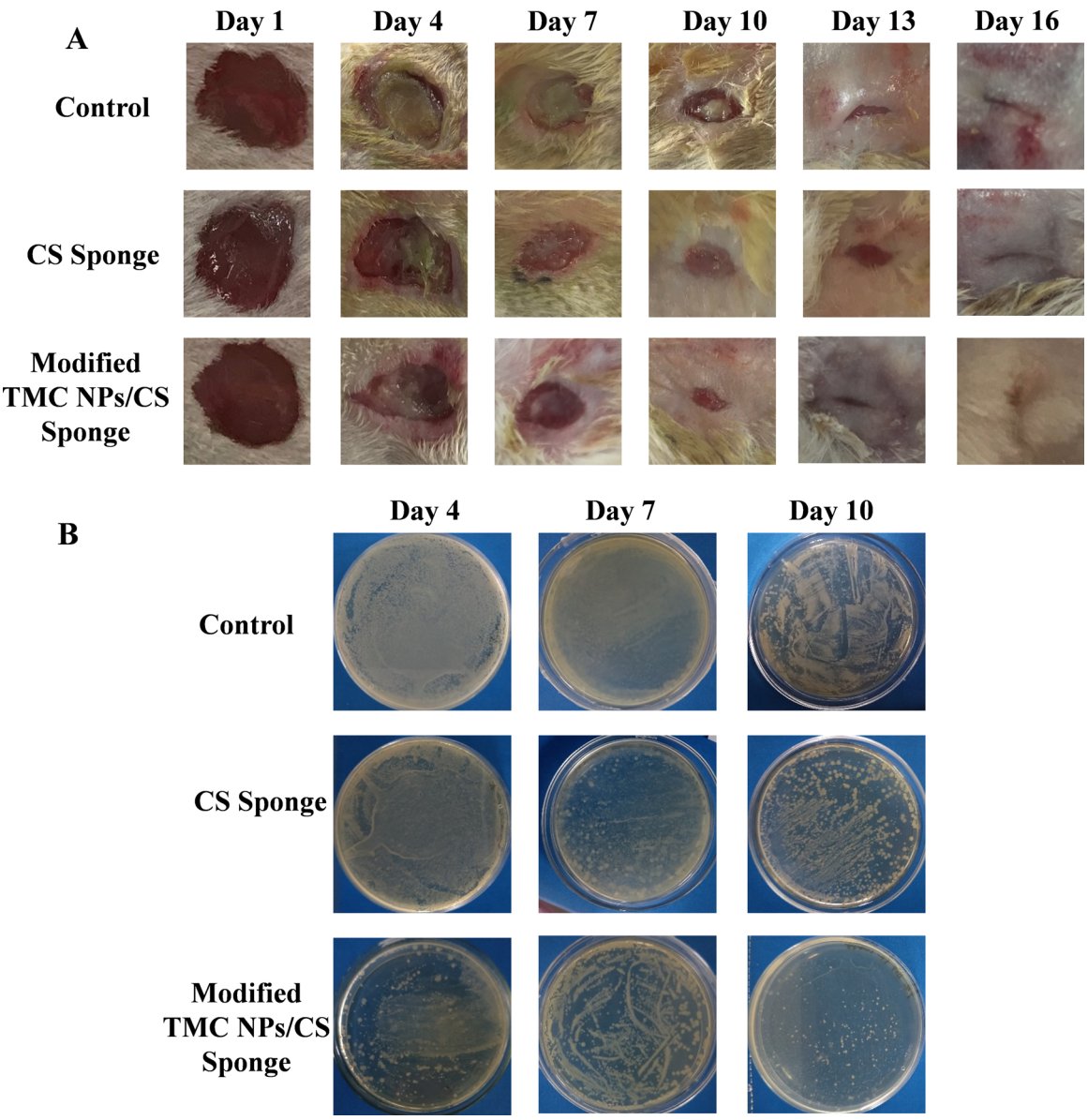

Fig. 8. Appearance of wounds in diabetic mice with bacterial infection. (A) Appearance of wounds on days 1, 4, 7, 10, 13 and 16. (B) Bacteria isolated from the mice wounds.

reactions appeared, so fewer inflammatory cells were found in the modified TMC NPs/CS sponge treatment group. As a result, less bacteria needed to be cleared in the wounds and less inflammatory reactions appeared, so fewer inflammatory cells were found in the modified TMC NPs/CS composite sponge treatment group. At day 10 post-wounding, microscopic investigation of the wound area treated with modified TMC NPs/CS composite sponge showed epithelization and granulation formation. Sebaceous gland was formed in the treatment modified TMC NPs/CS composite sponge group, while the wound area treated with the control and CS sponge did not show epithelization and granulation formation.

CS-based wound dressing materials attract a large number of researchers. As the wound dressing material, CS has different forms: sponges, hydrogels, fibers, nanoparticles and membranes (JAISWAL et al., 2013; Chen, Liu, Huang, Wang, & Fang, 2013; Mi et al., 2001; Wang, Zhu, Xue, & Wu, 2012; Xu, Weng, Gilkerson, Materon, & Lozano, 2015). An ideal chronic wound dressing material, should provide a moist wound environment, offer protection from secondary infections, remove wound exudate and promote tissue regeneration. Unlike acute wounds, chronic wounds should be dressed with adequate biomaterials in order to protect the long-term healing from contamination/infection, to prevent wound dissection (providing an ideal moist environment to help wound closure) (Moura, Dias, Carvalho, & Sousa, 2013). Sponge-type dressing as alternatives to hydrocolloid-type dressings for applications in chronic wounds attracts considerable attention. The sponge dressings are highly absorbent, cushioning, protective and conformable to body surfaces (Weller & Sussman, 2006). Moreover, they are easy to manipulate and can be adapted to the required wound size (Jeffcoate, Price, & Harding, 2010). In the study, modified TMC NPs/CS sponge showed the capacities of highly absorbent, high moisture retention, appropriate water vapor permeability and antibacterial activity, which could be used as an ideal dressing for chronic wounds.

3.6. In vivo anti-infection ability test

Unlike acute wounds, chronic wounds take a long time to heal, which should be dressed with adequate biomaterials in order to protect the long-term healing from contamination/infection. However, few studies have been conducted on wound dressing materials for chronic infected wounds. In the study, the anti-infection ability of the modified

TMC NPs/CS composite sponge was evaluated. The wounds were applied with *S. aureus* to mimic chronic infected wounds diabetic patients. The appearance of wounds with treatments of different materials in diabetic rats is recorded in Fig. 8. It can be seen that the progress of wound closure was notably improved with modified TMC NPs/CS composite sponge from day 4 onwards compared with gauze and CS sponge (Fig. 8A). On day 16 post-wounding, the healing rates of wounds treated with sponges or untreated were almost 100%, but only the wounds treated with the modified TMC NPs/CS composite sponges grew hairs, which indicated that only the wounds treated with the modified TMC NPs/CS composite sponges healed completely. Bacteria grow well no matter on sponge-treated or untreated wound at day 4. However, there is obvious decrease of the number of bacterial colonies on the modified TMC NPs/CS composite sponge treated wound, compared with the untreated and CS sponge-treated wounds at days 7 and 10 (Fig. 8B), which is probably attributed to the excellent antibacterial capacity of TMC NPs. It also well explains the phenomena that there is no obvious fester on the wound treated with modified TMC NPs/CS composite sponge, but it exists in untreated and CS sponge-treated wound. The rapid closure of infected wounds with modified TMC NPs/CS composite sponge clearly demonstrates their healing effectiveness for infected wounds on diabetic mice.

4. Conclusions

In this study, the asymmetrically wettable TMC NPs/CS composite sponge was prepared as the wound dressing material for treating chronic wounds. The optimum concentrations of TMC NPs and CS were 0.2 mg/mL and 2.0%, respectively. Asymmetric modification of stearic acid allows the upper surface of CS sponge hydrophobic and the opposite surface hydrophilic. The asymmetrically wettable CS sponge showed appropriate water vapor permeability, high porosity and enhanced moisture retention time, which is helpful for accelerating wound healing. The addition of TMC NPs enhanced the antibacterial activity of the CS sponge against gram-negative bacteria *E. coli* and gram-positive bacteria *S. aureus*. The hydrophobic surface displayed bacterial infiltration resistance and the hydrophilic surface could extensively absorb the exudates of wound and efficiently inhibit the growth of bacteria. The good biocompatibility of the asymmetrically wettable TMC NPs/CS composite sponge was identified with L929 cells after incubation with sponges for three days. *In vivo* wound healing evaluation in mice showed that the asymmetrically wettable TMC NPs/CS composite sponge possessed faster wound healing compared with the asymmetrically wettable CS sponge and gauze, and it also exhibited excellent re-epithelialization in histological observation. *In vivo* anti-infection study in mice illuminates the infected wounds treated with the modified TMC NPs/CS sponges healed faster due to the excellent antibacterial capacity of TMC NPs. In a conclusion, this composite sponge held great potential as the promising dressing material for chronic wounds.

Declaration of Competing Interest

There is no conflict of interests to declare.

Acknowledgements

This research was supported by Doctoral Scientific Fund Project of Weifang Medical University (grant number: 021811).

References

Anbazhagan, S., & Thangavelu, K. P. (2018). Application of tetracycline hydrochloride loaded-fungal chitosan and Aloe vera extract based composite sponges for wound dressing. *Journal of Advanced Research, 14*, 63–71.

Anisha, B. S., Sankar, D., Mohandas, A., Chennazhi, K. P., Nair, S. V., & Jayakumar, R. (2013). Chitosan–hyaluronan/nano chondroitin sulfate ternary composite sponges for medical use. *Carbohydrate Polymers, 92*(2), 1470–1476.

ASTM International, ASTM D882 (2012). *Standard test method for tensile properties of thin plastic sheeting.* Test method tensile prop. Thin Plast, Sheeting.

ASTM International (2016). *Standard test methods for water vapor transmission of materials.* Designation E96/E96M-16*Test methods water vap. Transm. Mater.*1–14.

Azuma, K., Izumi, R., Osaki, T., Ifuku, S., Morimoto, M., Saimoto, H., et al. (2015). Chitin, chitosan, and its derivatives for wound healing: Old and new materials. *Journal of Functional Biomaterials, 6*(1), 104–142.

Béduneau, A., Saulnier, P., & Benoit, J. P. (2007). Active targeting of brain tumors using nanocarriers. *Biomaterials, 28*(33), 4947–4967.

Bao, Z., Sun, Y., Rai, K., Peng, X., Wang, S., Nian, R., et al. (2018). The promising indicators of the thermal and mechanical properties of collagen from bass and tilapia: Synergistic effects of hydroxyproline and cysteine. *Biomaterials Science, 6*(11), 3042–3052.

Behrens, A. M., Sikorski, M. J., & Kofinas, P. (2014). Hemostatic strategies for traumatic and surgical bleeding. *Journal of Biomedical Materials Research Part A, 102*(11), 4182–4194.

Blackwell (2006). *Contact angle of liquid drops on solids. Surface chemistry of solid and liquid interfaces*. UK: Oxford.

Chen, C., Liu, L., Huang, T., Wang, Q., & Fang, Y. E. (2013). Bubble template fabrication of chitosan/poly(vinyl alcohol) sponges for wound dressing applications. *International Journal of Biological Macromolecules, 62*(11), 188–193.

Chen, Y., Li, J., Li, Q., Shen, Y., Ge, Z., Zhang, W., et al. (2016). Enhanced water-solubility, antibacterial activity and biocompatibility upon introducing sulfobetaine and quaternary ammonium to chitosan. *Carbohydrate Polymers, 143*, 246–253.

Fan, L., Yang, H., Yang, J., Peng, M., & Hu, J. (2016). Preparation and characterization of chitosan/gelatin/PVA hydrogel for wound dressings. *Carbohydrate Polymers, 146*, 427–434.

Feng, Y., Li, X., Zhang, Q., Yan, S., Guo, Y., Li, M., et al. (2019). Mechanically robust and flexible silk protein/polysaccharide composite sponges for wound dressing. *Carbohydrate Polymers, 216*, 17–24.

Fu, L., Zhang, J., & Yang, G. (2013). Present status and applications of bacterial cellulose-based materials for skin tissue repair. *Carbohydrate Polymers, 92*(2), 1432–1442.

Gao, P., Xia, G., Bao, Z., Feng, C., Cheng, X., Kong, M., et al. (2016). Chitosan based nanoparticles as protein carriers for efficient oral antigen delivery. *International Journal of Biological Macromolecules, 91*, 716–723.

Ghavaminejad, A., Park, C. H., & Kim, C. S. (2016). In situ synthesis of antimicrobial silver nanoparticles within antifouling zwitterionic hydrogels by catecholic redox chemistry for wound healing application. *Biomacromolecules, 17*(3), 1213–1223.

Hernandez-Rangel, A., Silva-Bermudez, P., Espana-Sanchez, B. L., Luna-Hernandez, E., Almaguer-Flores, A., Ibarra, C., et al. (2019). Fabrication and in vitro behavior of dual-function chitosan/silver nanocomposites for potential wound dressing applications. *Materials Science & Engineering C-Materials for Biological Applications, 94*, 750–765.

Hinman, C. D., & Maibach, H. (1963). Effcet of air exposure and occlusion on experimental human skin wounds. *Nature, 200*(4904), 377–378.

Hu, S., Bi, S., Yan, D., Zhou, Z., Sun, G., Cheng, X., et al. (2018). Preparation of composite hydroxybutyl chitosan sponge and its role in promoting wound healing. *Carbohydrate Polymers, 184*, 154–163.

Huang, K. T., Fang, Y. L., Hsieh, P. S., Li, C. C., Dai, N. T., & Huang, C. J. (2017). Non-sticky and antimicrobial zwitterionic nanocomposite dressings for infected chronic wounds. *Biomaterials Science, 5*(6), https://doi.org/10.1039/C1037BM00039A.

Huang, R., Chen, G., Sun, M., Hu, Y., & Gao, C. (2006). Studies on nanofiltration membrane formed by diisocyanate cross-linking of quaternized chitosan on poly(acrylonitrile) (PAN) support. *Journal of Membrane Science, 286*(1-2), 237–244.

ISO (2009). *Biological evaluation of medical devices, part 5: Tests for in vitro cytotoxicity. ISO 10993-5*. Geneva, Switzerland: ISO.

Ivanova, N. A., & Philipchenko, A. B. (2012). Superhydrophobic chitosan-based coatings for textile processing. *Applied Surface Science, 263*(24), 783–787.

Jaiswal, M., Gupta, A., Agrawal, A., Jassal, K., Dinda, M., & Kr, A. (2013). Bi-layer composite dressing of gelatin nanofibrous mat and poly vinyl alcohol hydrogel for drug delivery and wound healing application: In-vitro and in-vivo studies. *Journal of Biomedical Nanotechnology, 9*(9), 1495–1508.

Jayakumar, R., Prabaharan, M., Sudheesh Kumar, P. T., Nair, S. V., & Tamura, H. (2011). Biomaterials based on chitin and chitosan in wound dressing applications. *Biotechnology Advances, 29*(3), 322–337.

Jeffcoate, W. J., Price, P., & Harding, K. G. (2010). Wound healing and treatments for people with diabetic foot ulcers. *Diabetes/metabolism Research and Reviews, 20*(S1), S78–S89.

Kempf, M., Miyamura, Y., & Liu, P. Y. (2011). A denatured collagen microfiber scaffold seeded with human fibroblasts and keratinocytes for skin grafting. *Biomaterials, 32*(21), 4782–4792.

Khorasani, M. T., Joorabloo, A., Moghaddam, A., Shamsi, H., & MansooriMoghadam, Z. (2018). Incorporation of ZnO nanoparticles into heparinised polyvinyl alcohol/chitosan hydrogels for wound dressing application. *International Journal of Biological Macromolecules, 114*, 1203–1215.

Kong, M., Chen, X. G., Xing, K., & Park, H. J. (2010). Antimicrobial properties of chitosan and mode of action: A state of the art review. *International Journal of Food Microbiology, 144*(1), 51–63.

Kumar, P. T. S., Abhilash, S., Manzoor, K., Nair, S. V., Tamura, H., & Jayakumar, R. (2010). Preparation and characterization of novel β-chitin/nanosilver composite scaffolds for wound dressing applications. *Carbohydrate Polymers, 80*(3), 761–767.

Lee, Y., Jin, W. B., Dong, H. O., Park, K. M., Chun, Y. W., Sung, H. J., et al. (2013). In situ forming gelatin-based tissue adhesives and their phenolic content-driven properties. *Journal of Materials Chemistry B, 1*(18), 2407–2414.

Li, J., Xie, B., Xia, K., Zhao, C., Li, Y., Li, D., et al. (2018). Facile synthesis and characterization of cross-linked chitosan quaternary ammonium salt membrane for antibacterial coating of piezoelectric sensors. *International Journal of Biological Macromolecules, 120*, 745–752.

Li, Q., Lu, F., Zhou, G., Yu, K., Lu, B., Xiao, Y., et al. (2017). Silver Inlaid with Gold Nanoparticle/Chitosan Wound Dressing Enhances Antibacterial Activity and Porosity, and Promotes Wound Healing. *Biomacromolecules, 18*(11), 3766–3775.

Liang, D., Lu, Z., Yang, H., Gao, J., & Chen, R. (2016). Novel asymmetric wettable AgNPs/Chitosan wound dressing: In vitro and in vivo evaluation. *ACS Applied Materials & Interfaces, 8*(6), 3958–3968.

Lima, L. L., Taketa, T. B., Beppu, M. M., Sousa, I. M. O., Foglio, M. A., & Moraes, A. M. (2019). Coated electrospun bioactive wound dressings: Mechanical properties and ability to control lesion microenvironment. *Materials Science and Engineering C, 100*, 493–504.

Liu, Y., Xin, J. H., & Choi, C. H. (2012). Cotton fabrics with single-faced superhydrophobicity. *Langmuir the ACS Journal of Surfaces & Colloids, 28*(50), 17426–17434.

Lu, Z., Gao, J., He, Q., Wu, J., Liang, D., Yang, H., et al. (2017). Enhanced antibacterial and wound healing activities of microporous chitosan-Ag/ZnO composite dressing. *Carbohydrate Polymers, 156*, 460–469.

Ma, R., Wang, Y., Qi, H., Shi, C., Wei, G., Xiao, L., et al. (2019). Nanocomposite sponges of sodium alginate/graphene oxide/polyvinyl alcohol as potential wound dressing: In vitro and in vivo evaluation. *Composites Part B Engineering, 167*, 396–405.

Masood, N., Ahmed, R., Tariq, M., Ahmed, Z., Masoud, M. S., Ali, I., et al. (2019). Silver nanoparticle impregnated chitosan-PEG hydrogel enhances wound healing in diabetes induced rabbits. *International Journal of Pharmaceutics, 559*, 23–36.

Mcdaniel, J. C., & Browning, K. K. (2014). Smoking, chronic wound healing, and implications for evidence-based practice. *Journal of WOCN, 41*(5), 415–423.

Mi, F. L., Shyu, S. S., Wu, Y. B., Lee, S. T., Shyong, J. Y., & Huang, R. N. (2001). Fabrication and characterization of a sponge-like asymmetric chitosan membrane as a wound dressing. *Biomaterials, 22*(2), 165–173.

Minami, S. (1997). Mechanism of wound healing acceleration by Chitin and Chitosan. *The Japanese Journal of Veterinary Research, 44*(1), 218–219.

Moroz, A., & Deffune, E. (2013). Platelet-rich plasma and chronic wounds: Remaining fibronectin may influence matrix remodeling and regeneration success. *Cytotherapy, 15*(11), 1436–1439.

Moura, L. I. F., Dias, A. M. A., Carvalho, E., & Sousa, H. C. D. (2013). Recent advances on the development of wound dressings for diabetic foot ulcer treatment—A review. *Acta Biomaterialia, 9*(7), 7093–7114.

Murakami, K., Aoki, H., Nakamura, S., Nakamura, S., Takikawa, M., Hanzawa, M., et al. (2010). Hydrogel blends of chitin/chitosan, fucoidan and alginate as healing-impaired wound dressings. *Biomaterials, 31*(1), 83–90.

Ong, S. Y., Wu, J., Moochhala, S. M., Tan, M. H., & Lu, J. (2008). Development of a chitosan-based wound dressing with improved hemostatic and antimicrobial properties. *Biomaterials, 29*(32), 4323–4332.

Ordikhani, F., Tamjid, E., & Simchi, A. (2014). Characterization and antibacterial performance of electrodeposited chitosan-vancomycin composite coatings for prevention of implant-associated infections. *Materials Science and Engineering C, 41*, 240–248.

Pawar, V., Bulbake, U., Khan, W., & Srivastava, R. (2019). Chitosan sponges as a sustained release carrier system for the prophylaxis of orthopedic implant-associated infections. *International Journal of Biological Macromolecules, 134*, 100–112.

Jiang, Q., Shun-Bin Wang, Z.-H. C., & Chen, X.-D. (2017). Comparative effectiveness of different wound dressings for patients with partial-thickness burns: study protocol of a systematic review and a Bayesian framework network meta-analysis. *BMJ Open, 7*, e013289.

Queen, D., Gaylor, J. D. S., Evans, J. H., Courtney, J. M., & Reid, W. H. (1987). The preclinical evaluation of the water vapour transmission rate through burn wound dressings. *Biomaterials, 8*(5), 367–371.

Sacco, P., Travan, A., Borgogna, M., Paoletti, S., & Marsich, E. (2015). Silver-containing antimicrobial membrane based on chitosan-TPP hydrogel for the treatment of wounds. *Journal of Materials Science Materials in Medicine, 26*(3), 128.

Sanad, A. B., & Abdel-Bar, H. M. (2017). Chitosan–hyaluronic acid composite sponge scaffold enriched with Andrographolide-loaded lipid nanoparticles for enhanced wound healing. *Carbohydrate Polymers, 173*, 441–450.

Sasaki, K., Tenjimbayashi, M., Manabe, K., & Shiratori, S. (2016). Asymmetric Superhydrophobic/Superhydrophilic cotton fabrics designed by spraying polymer and nanoparticles. *ACS Applied Materials & ISnterfaces, 8*(1), 651–659.

Schneider, A., Wang, X. Y., Kaplan, D. L., Garlick, J. A., & Egles, C. (2009). Biofunctionalized electrospun silk mats as a topical bioactive dressing for accelerated wound healing. *Acta Biomaterialia, 5*(7), 2570–2578.

Schrand, A. M., Rahman, M. F., Hussain, S. M., Schlager, J. J., Smith, D. A., & Syed, A. F. (2010). Metal-based nanoparticles and their toxicity assessment. *Wiley Interdisciplinary Reviews-Nanomedicine and Nanobiotechnology, 2*(5), 544–568.

Shen, L., Wang, B., Wang, J., Fu, J., Picart, C., & Ji, J. (2012). Asymmetric free-standing film with multifunctional anti-bacterial and self-cleaning properties. *ACS Applied Materials & Interfaces, 4*(9), 4476–4483.

Tan, H., Ma, R., Lin, C., Liu, Z., & Tang, T. (2013). Quaternized chitosan as an antimicrobial agent: Antimicrobial activity, mechanism of action and biomedical applications in orthopedics. *International Journal of Molecular Sciences, 14*(1), 1854–1869.

Vallapa, N., Wiarachai, O., Thongchul, N., Pan, J., Tangpasuthadol, V., Kiatkamjornwong, S., et al. (2011). Enhancing antibacterial activity of chitosan surface by heterogeneous quaternization. *Carbohydrate Polymers, 83*(2), 868–875.

Wang, J., Xu, M., Cheng, X., Kong, M., Liu, Y., Feng, C., et al. (2016). Positive/negative surface charge of chitosan based nanogels and its potential influence on oral insulin delivery. *Carbohydrate Polymers, 136*, 867–874.

Wang, T., Zhu, X. K., Xue, X. T., & Wu, D. Y. (2012). Hydrogel sheets of chitosan, honey and gelatin as burn wound dressings. *Carbohydrate Polymers, 88*(1), 75–83.

Wang, Y., Wang, C., Xie, Y., Yang, Y., Zheng, Y., Meng, H., et al. (2019). Highly transparent, highly flexible composite membrane with multiple antimicrobial effects used for promoting wound healing. *Carbohydrate Polymers, 222*, 114985.

Weller, C., & Sussman, G. (2006). Wound dressings update. *Journal of Pharmacy Practice and Research, 36*(4), 318–324.

Wu, S. C., Driver, V. R., Wrobel, J. S., & Armstrong, D. G. (2007). Foot ulcers in the diabetic patient, prevention and treatment. *Vascular Health and Risk Management, 3*(1), 65–76.

Xia, G., Lang, X., Kong, M., Cheng, X., Liu, Y., Feng, C., et al. (2016). Surface fluid-swellable chitosan fiber as the wound dressing material. *Carbohydrate Polymers, 136*, 860–866.

Xia, G., Liu, Y., Tian, M., Gao, P., Bao, Z., Bai, X., et al. (2017). Nanoparticles/thermosensitive hydrogel reinforced with chitin whiskers as a wound dressing for treating chronic wounds. *Journal of Materials Chemistry B, 5*(17), 3172–3185.

Xie, Y., Liu, X., & Qiang, C. (2007). Synthesis and characterization of water-soluble chitosan derivate and its antibacterial activity. *Carbohydrate Polymers, 69*(1), 142–147.

Xu, F., Weng, B., Gilkerson, R., Materon, L. A., & Lozano, K. (2015). Development of tannic acid/chitosan/pullulan composite nanofibers from aqueous solution for potential applications as wound dressing. *Carbohydrate Polymers, 115*, 16–24.

Xu, R., Xia, H., He, W., Li, Z., Zhao, J., Liu, B., et al. (2016). Controlled water vapor transmission rate promotes wound-healing via wound re-epithelialization and contraction enhancement. *Scientific Reports, 6*, 24596.

Zhou, Z., Hu, F., Hu, S., Kong, M., Feng, C., Liu, Y., et al. (2018). pH-Activated nanoparticles with targeting for the treatment of oral plaque biofilm. *Journal of Materials Chemistry B, 6*(4), 586–592.

Zhou, Z., Yan, D., Cheng, X., Kong, M., Liu, Y., Feng, C., et al. (2016). Biomaterials based on N,N,N-trimethyl chitosan fibers in wound dressing applications. *International Journal of Biological Macromolecules, 89*, 471–476.